Traffic flow and $1/f$ fluctuations

M.Y. Choi and H.Y. Lee
Department of Physics and Center for Theoretical Physics, Seoul National University, Seoul 151-742, Korea
(Received 23 March 1995; revised manuscript received 29 August 1995)

We study the traffic flow in the hydrodynamic limit, where the analogy to fluid flow leads to the traffic equation in the form of the Navier-Stokes equation. It is shown that the traffic equation exhibits a variety of behaviors such as homogeneous flow, turbulent behavior, and density waves with fluctuations in the appropriate regime. In particular, the stability against random fluctuations and the possibility of $1/f$ fluctuations in the traffic current are investigated.

PACS number(s): 05.40.+j, 47.54.+r, 89.40.+k, 81.35.+k

I. INTRODUCTION

Traffic flow on a real road displays a variety of behaviors such as clustering and $1/f$ fluctuations [1]; the ubiquitous appearance of the latter in many diverse systems has been a source of mystery [2]. In general, there have been two distinct approaches that attempt to describe such collective properties of traffic flow. One is the cellular automaton approach, in which cars are treated as distinguishable particles, the roads are expressed as discrete lattices, and the system evolves in discrete time steps with given rules [3,4]. On the other hand, it is usually expected that some essential features of fairly heavy traffic flow may be obtained by treating a stream of traffic as a continuum with the density and the current, which represent the number of cars per unit length and the number of cars crossing the position per unit time, respectively [5]. In this hydrodynamic description, traffic flow is described by the continuity equation (conservation of mass) together with the equation of motion (conservation of momentum), and the analogy between traffic flow and fluid flow naturally leads to the traffic equation in the form [6]

$$\frac{\partial \rho}{\partial t} + \frac{\partial}{\partial x}\rho v = 0,$$

$$\rho\left[\frac{\partial v}{\partial t} + v\frac{\partial v}{\partial x}\right] = \frac{\partial}{\partial x}\left(\mu\frac{\partial v}{\partial x}\right) - \frac{\partial p}{\partial x} + \frac{\rho}{\tau}[V(\rho) - v], \quad (1)$$

where $\rho(x,t)$ is the density of cars at position x (on the road) at time t, p is the local pressure given by $p = \rho c_0^2$ with c_0^2 denoting the effective "temperature" of the system or the variance of the velocity distribution [5,6], and μ is the viscosity. On the road drivers control the speed v and tend to adjust it to the maximal safe value $V(\rho)$, which is a phenomenological function of the density. $V(\rho)$ depends on the traffic regulations, road conditions, etc., and is determined empirically. Thus the last term on the right-hand side of Eq. (1) represents the relaxation effects with the relaxation time τ, reflecting the two essential processes: acceleration and slowing down.

Equation (1) indeed exhibits spontaneous formation of a cluster of cars in an initially homogeneous traffic flow, if the density of cars exceeds some critical value [6]. Such a cluster of cars, where the density of cars is high and the average velocity is low, can move with constant velocity in the direction or in the opposite direction of the flow, depending on the parameters and initial conditions. The appearance of the cluster has been shown to result from the competition between active processes, which tend to increase the amplitude of nonhomogeneous perturbations, and the damping processes that suppress it. The active processes are related to the character of the function $V(\rho)$ while the damping processes are connected with the the diffusion (viscosity) process. It has been further shown, via the linear stability analysis, that the homogeneous state described by Eq. (1) is unstable against long-wavelength perturbations if $[\rho_0 V'(\rho_0)^2 - c_0^2/\rho_0] > 0$, where ρ_0 is the average density and $V'(\rho) \equiv \partial V(\rho)/\partial\rho$ [7]. Nevertheless, the interesting possibility of complex behaviors such as $1/f$ fluctuations and chaotic flow has not been addressed to our knowledge.

The purpose of this paper is to examine the possibility of such complex behaviors in the traffic flow modeled by Eq. (1), together with their stability against random fluctuations. For that purpose, we notice that there exist similar features between the granular flow and the traffic flow with the cars taking the role of granular particles. Indeed the similarity between Eq. (1) and the equation describing the void motion in granular flow under tapping has been pointed out [8]; in the granular flow, where both the dissipation among the granular particles and the roughness of the walls of pipes are essential to the formation of density waves, the power spectrum of density fluctuations has been found to take the form $1/f^\alpha$ with α close to 4/3 [9]. We thus take into account the granular nature of traffic flow, and investigate in detail its effects on the traffic flow described by Eq. (1). To consider the granular nature, we introduce a cutoff in the density, which corresponds to the maximum density of cars on the road [6]. The resulting traffic equation exhibits a variety of interesting behaviors such as homogeneous (laminar) flow, chaotic flow, and density waves. In particular, $1/f$ fluctuations are also found to exist in the traffic flow, which depends on the shape of the function $V(\rho)$ such as

the existence of a cutoff or a large slope.

This paper consists of four sections: Section II presents the detailed behavior of the traffic equation with the cutoff. According to the values of the Lyapunov exponent, the chaotic phase as well as the density-wave phase is identified, and typical time evolutions of the density are shown. The phase diagram in the (ρ_0, c_0) plane exhibits the homogeneous phase with the laminar flow, the chaotic phase with the irregular flow, and the density-wave phase with traveling density waves. The power spectra of the current fluctuations are also computed, which shows $1/f$ fluctuations in the density-wave phase. In contrast, the chaotic phase does not display $1/f$ fluctuations as expected. Section III is devoted to the long-wave analysis of the traffic equation, which reveals that the chaotic behavior arises from the instability in the second-order corrections. Finally, Sec. IV summarizes the main results.

II. PHASE DIAGRAMS AND $1/f$ FLUCTUATIONS

We perform numerical integration of the discrete version of Eq. (1), introducing the cutoff density ρ_c, with respect to which the density is measured [6]. We further rescale the time and the length in units of τ and $\ell \equiv \sqrt{\mu\tau/\rho_c}$, respectively, and measure v, $V(\rho)$, and c_0 in units of ℓ/τ [6]. For the numerical integration, we discretize the road into L positions $x = n$ (in units of ℓ), and write Eq. (1) in the dimensionless form

$$\frac{\partial \rho(n,t)}{\partial t} = -\frac{1}{2}\left[j(n+1,t) - j(n-1,t)\right],$$
$$\frac{\partial j(n,t)}{\partial t} = \left[v(n+1,t) + v(n-1,t) - 2v(n,t)\right] - \frac{1}{2}c_0^2\left[\rho(n+1,t) - \rho(n-1,t)\right] + \rho(n,t)\left\{V[\rho(n,t)] - v(n,t)\right\}$$
$$-\frac{1}{2}j(n,t)\left[v(n+1,t) - v(n-1,t)\right] - \frac{1}{2}v(n,t)\left[j(n+1,t) - j(n-1,t)\right], \qquad (2)$$

where the current is given by $j(n,t) \equiv \rho(n,t)v(n,t)$. We choose the initial conditions that the density and the velocity are perturbed randomly about the homogeneous state $\rho = \rho_0$ and $v = v_0 \equiv V(\rho_0)$, which mimic the realistic situation. Presumably, small density fluctuations are distributed randomly on the highway; we thus assign uniform random numbers $\delta\rho(x,0)$ and $\delta v(x,0)$ in the range $[-0.01, 0.01]$ to each position x, leading to the initial conditions $\rho(x,0) = \rho_0 + \delta\rho(x,0)$ and $v(x,0) = v_0 + \delta v(x,0)$. We also take the periodic boundary conditions $\rho(x+L) = \rho(x)$ and $v(x+L) = v(x)$, which correspond to a highway loop of length L. Finally, the cutoff procedure works in the following way: When the density $\rho(n)$ at site n exceeds the cutoff density $\rho_c \equiv 1$, then $\rho(n)$ and $v(n)$ are set equal to ρ_c and zero, respectively, $\rho(n) - \rho_c$ is added to the density $\rho(n-1)$ at the backward neighboring site $n-1$, and $v(n-1)$ is replaced by $v(n-1)\rho(n-1)/[\rho(n-1) + \rho(n) - \rho_c]$.

The average relaxation velocity profile $V(\rho)$ in Eq. (2) is expected to be a smooth and decreasing function of ρ. Here we consider several simple forms for $V(\rho)$ instead of determining it empirically. One of the specific (dimensionless) forms considered mainly is given by

$$V(\rho) = \frac{1}{1+\beta\rho^2}, \qquad (3)$$

where we choose $\beta = 4$ for simplicity. Other forms that have been considered include $V(\rho) = e^{-a\rho}$, $\exp(-a\rho^2)$, $A\{1 + \exp[a(\rho - b)]\}^{-1}$, $\exp(-a\rho^2)(1-\rho)^b(1-\rho^2/2)$, and $[A\exp(-a\rho^n) + (1-A)](1-\rho)^b$. Equation (2) together with Eq. (3) [or with other forms of $V(\rho)$] is integrated by the second-order Runge-Kutta method [10] with the time interval $\Delta t = 0.01$.

As a result, two qualitatively different states are found to exist in the unstable region. One is the chaotic state displaying a positive Lyapunov exponent ($\lambda = 0.08 \pm 0.01$) [Fig. 1(a)]. In this chaotic phase, the value of den-

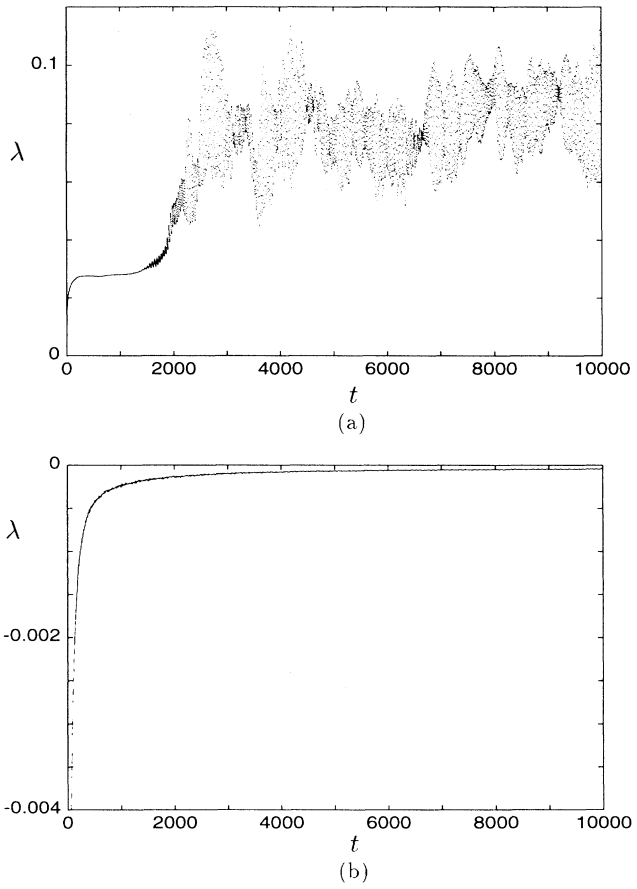

FIG. 1. Lyapunov exponents for the time evolution of the density in the system of size $L = 400$ for (a) $\rho_0 = 0.35$ and $c_0 = 0.35$; (b) $\rho_0 = 0.45$ and $c_0 = 0.35$. In (a), the Lyapunov exponent is positive, indicating a chaotic phase. In contrast, (b) corresponds to the (nonchaotic) density-wave phase.

sity does not reach ρ_c, and accordingly the cutoff procedure does not operate. The corresponding pattern of the density evolution is revealed in Fig. 2(a), which displays the ten stationary-state density profiles taken in the increments of 10^4 time steps. The other is the density-wave phase that is affected by the cutoff. It appears as the density is increased for a given (not too large) value of c_0, and displays the negative Lyapunov exponent which approaches zero, as shown in Fig. 1(b). The corresponding pattern of the density evolution [Fig. 2(b)], displaying density profiles in increments of 10^3 time steps, also exhibits features different from those of the chaotic phase: While the clusters (high-density regions) in (a) evolve irregularly, (b) displays density waves traveling with small fluctuations, in the direction opposite to that of the flow. The phase boundary between the two phases can be obtained by computing the values of ρ_0 and c_0, for which the maximum value of density reaches the cutoff density ρ_c, which yields the phase diagram shown in Fig. 3.

We next calculate the power spectrum of traffic currents, using the fast Fourier transform routine with the Parzen window and averaging processes [10]. We consider a system of length $L = 800$, and allow the dynamic process to evolve for very long time steps. Thus, with 26 214 400 computing time steps, we obtain 131 072 data points, the time series of which is broken into 32 segments. A representative power spectrum in the density-wave region of the system of $L = 800$ is shown in Fig. 4(a), where a peak around $f = 300$ can be observed. Such a peak is due to the contribution of the high-density pulse traveling periodically in the system [Fig. 2(b)]. Apart from this peak, Fig. 4(a) exhibits the power-law regime, where the spectrum falls off as $1/f^{\alpha}$. Here the length of the time series of the data sets limits to the low-frequency range. Nevertheless the power-law behavior can be observed at frequencies as low as $f \approx 4$. The dashed line represents the least-square fit to the data between $f = 30$ and 150, which yields the exponent $\alpha = 1.09 \pm 0.09$. Within the range investigated, the exponent α is found to be independent of the values of the parameters; the position of the peak, on the other hand, depends on the values. To check the size dependence, we have also considered the systems of $L = 400$ and 1600: With the same values of the parameters, these systems yield the exponent $\alpha = 1.17 \pm 0.09$ and 1.12 ± 0.07, which apparently indicates that the power-law behavior is not merely a finite-size effect. It is thus concluded that the density-wave phase exhibits $1/f$ fluctuations, which have been observed on real highways [1]. In contrast, the chaotic phase does not display $1/f$ fluctuations. Figure 4(b) shows a typical power spectrum in the chaotic phase, which does not possess the power-law regime at low frequencies. The power-law behavior appears in the rather restricted range at high frequencies ($f \geq 50$), with a

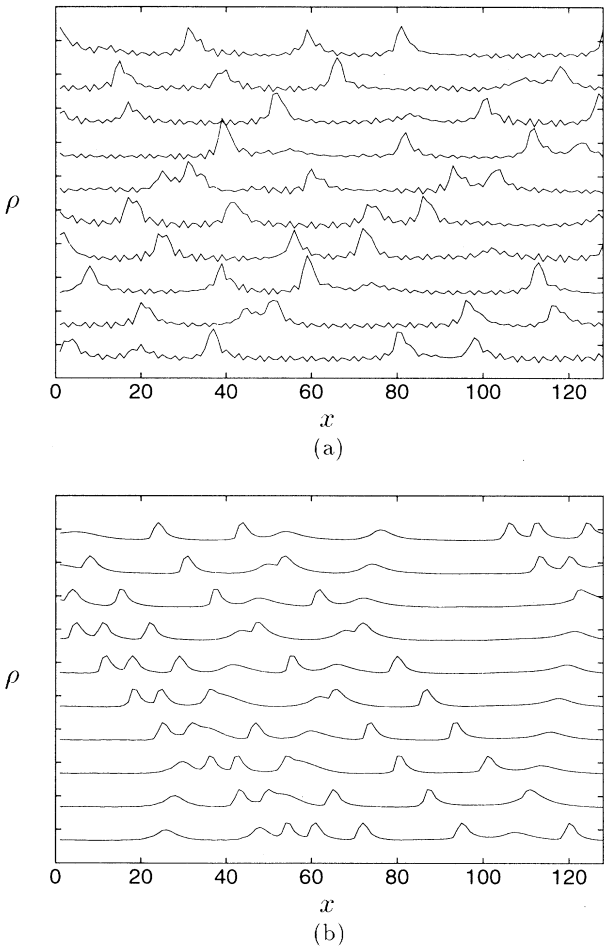

FIG. 2. Time evolution of the density for (a) $\rho_0 = 0.35$ and $c_0 = 0.35$; (b) $\rho_0 = 0.45$ and $c_0 = 0.35$. The ten curves (from the bottom to the top) in each of (a) and (b) represent the stationary-state density profiles taken in the increments of (a) 10^4 and (b) 10^3 time steps, respectively. In (a), the clusters (high-density regions) evolve irregularly, whereas (b) displays density waves traveling with small fluctuations, in the direction opposite to that of the flow.

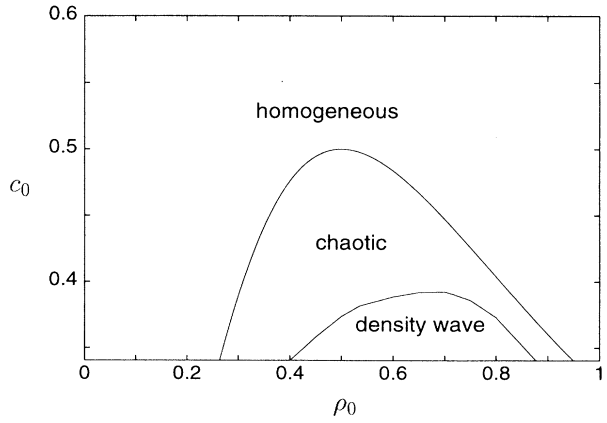

FIG. 3. Phase diagram of the traffic equation on the (ρ_0, c_0) plane, showing the homogeneous (laminar) flow, the chaotic phase, and the density-wave phase. For not too large c_0, the amplitude of the cluster grows with ρ_0, resulting in the operation of the cutoff mechanism.

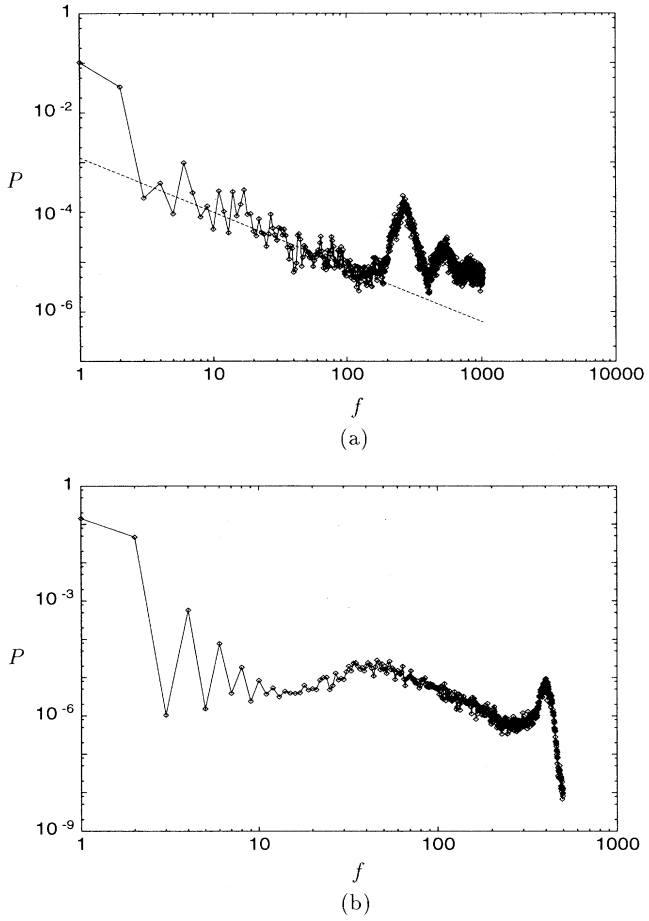

FIG. 4. Power spectrum of traffic currents at $x = 400$ in the system of size $L = 800$ for $c_0 = 0.3$ and (a) $\rho_0 = 0.75$; (b) $\rho_0 = 0.3$. Case (a) corresponds to the density-wave phase, and the dashed line represents the least-square fit with the slope -1.09 ± 0.09. In (b), which corresponds to the chaotic phase, the spectrum is more or less white.

larger value of the exponent: $\alpha = 2.06 \pm 0.08$. Except for this, the power spectrum apparently displays fluctuations of the white-spectrum type. We have also measured the power spectrum of density fluctuations in the system with the same parameters, and obtained $\alpha = 1.38 \pm 0.08$ in the density wave phase and the white spectrum in the chaotic phase.

Among other forms of $V(\rho)$ considered, $\exp(-a\rho^2)(1-\rho)^b(1-\rho^2/2)$ and $[A\exp(-a\rho^n)+(1-A)](1-\rho)^b$ with small b, as well as $e^{-a\rho}$ with the cutoff,

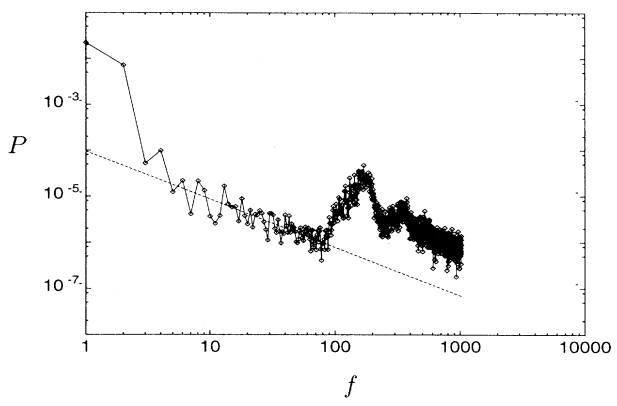

FIG. 5. Power spectrum of traffic currents at $x = 400$ in the system of size $L = 800$, with $V(\rho) = [0.8\exp(-4\rho^2) + 0.2](1-\rho)^{0.001}$ for $c_0 = 0.2$ and $\rho_0 = 0.75$. The least-square fits represented by the dashed lines have the slope -1.05 ± 0.07.

lead to behaviors largely similar to those displayed by Eq. (3). The typical power spectrum in the system with $V(\rho) = [A\exp(-a\rho^n)+(1-A)](1-\rho)^b$ is shown in Fig. 5 for $A = 0.8$, $n = 2$, $a = 4$, and $b = 0.001$, which yields the exponent $\alpha = 1.05 \pm 0.07$. On the other hand, the above forms of $V(\rho)$ with large b as well as $A\{1+\exp[a(\rho-b)]\}^{-1}$ in general do not lead to $1/f$ fluctuations. This indicates that the appearance of density waves and $1/f$ fluctuations depends on the slope of $V(\rho)$ at ρ_c. In particular $V(\rho)$ approaching zero with a small slope at ρ_c does not exhibit $1/f$ fluctuations: Here random fluctuations eventually destroy the density waves, resulting in chaotic evolution.

III. LONG-WAVE ANALYSIS

The long-wave analysis has been applied to the traffic equation, which is slightly different from Eq. (1) in the viscosity term, to demonstrate the existence of soliton solutions [7]. Here the method applied to Eq. (1) reveals the chaotic behavior arising from the instability. Following Ref. [7], we set

$$\rho(x,t) = \rho_0 + \epsilon^2\hat{\rho}(\epsilon x, \epsilon^3 t),$$
$$v(x,t) = v_0 + \epsilon^2\hat{v}(\epsilon x, \epsilon^3 t), \tag{4}$$

where ϵ is a small number, and write Eq. (1) as follows:

$$\hat{\rho}_t + \mu\tau V'(\rho_0)\hat{\rho}_{xxx} + [2V'(\rho_0) + \rho_0 V''(\rho_0)]\,\hat{\rho}\hat{\rho}_x = -\epsilon\tau\rho_0\left\{2\mu\tau[V'(\rho_0)]^2\hat{\rho}_{xx} + \alpha\hat{\rho} + \frac{1}{2}\left\{[V'(\rho_0)]^2 + 2\rho_0 V'(\rho_0)V''(\rho) - c_0^2 f''(\rho_0)\right\}\hat{\rho}^2\right\}_{xx} + \epsilon^2\left[\frac{\tau\mu V'(\rho_0)}{\rho_0}\hat{\rho}_{xxx}\hat{\rho} - \frac{V''(\rho_0)}{2}\hat{\rho}^2\hat{\rho}_x\right] + O(\epsilon^3), \tag{5}$$

where $f(\rho) \equiv \ln\rho$, $\alpha \equiv (1/\epsilon^2)\{\rho_0[V'(\rho_0)]^2 - c_0^2 f'(\rho_0)\}$, and the subscript denotes the derivative with respect to that variable.

For convenience, we put

$$\hat{\rho} = \frac{3\mu}{2\tau V'(\rho_0)[2V'(\rho_0)+\rho_0 V''(\rho_0)]}\tilde{\hat{\rho}},$$
$$x = -2\tau V'(\rho_0)\tilde{x},$$
$$t = \frac{8\tau^2}{\mu}[V'(\rho_0)]^2\tilde{t},$$

and, for simplicity, drop the tildes on the new variables $\tilde{x}$, $\tilde{t}$, and $\tilde{\hat{\rho}}$, which leads to Eq. (5) in the form

$$\hat{\rho}_t - \hat{\rho}_{xxx} - 6\hat{\rho}\hat{\rho}_x = -\epsilon\left[\frac{2\tau\rho_0\alpha}{\mu}\hat{\rho}_{xx} + \rho_0\hat{\rho}_{xxxx} + a(\hat{\rho}\hat{\rho}_x)_x\right] - \epsilon^2\left\{\frac{3\mu}{2\tau V'(\rho_0)[2V'(\rho_0)+\rho_0V''(\rho_0)]}\hat{\rho}_{xxx}\hat{\rho} - \frac{9\mu V''(\rho_0)}{2\tau V'(\rho_0)[2V'(\rho_0)+\rho_0V''(\rho_0)]^2}\hat{\rho}^2\hat{\rho}_{xx}\right\} \quad (6)$$

with

$$a \equiv \frac{3\rho_0[V'(\rho_0)^2 + 2\rho_0V'(\rho_0)V''(\rho_0) - c_0^2 f''(\rho_0)]}{V'(\rho_0)[2V'(\rho_0)+\rho_0V''(\rho_0)]}.$$

The solution of Eq. (6) to leading order takes the form [11]

$$\hat{\rho} = 2k^2\mathrm{sech}^2k(x - x_0 + 4k^2t) \equiv u(x,t,k,x_0), \quad (7)$$

where k is a free parameter. To the order ϵ, we thus have

$$\hat{\rho} = u(x,t,k,x_0) + \epsilon\hat{\rho}_1, \quad (8)$$

where k and x_0 have been assumed to vary with the slow time variable $t_1 = \epsilon t$. We insert this into the evolution equation (6), and obtain

$$\frac{\partial u}{\partial k}\frac{dk}{dt_1} + \frac{\partial u}{\partial x_0}\frac{dx_0}{dt_1} + A\hat{\rho}_1 = -\left[\frac{2\tau\rho_0}{\mu}\alpha u_{xx} + \rho_0 u_{xxxx} + a(uu_x)_x\right] \quad (9)$$

where the operator A is defined to be

$$A\hat{\rho}_1 \equiv \left[\frac{\partial}{\partial t} - \frac{\partial^3}{\partial x^3} - 6\frac{\partial^3}{\partial x^3}u\right]\hat{\rho}_1.$$

Here we have $dk/dt_1 = 0$ if

$$k^2 = \frac{7\tau}{2\mu}\alpha\left[\frac{V'(\rho_0)[2V'(\rho_0)+\rho_0V''(\rho_0)]}{4[V'(\rho_0)]^2 - 7\rho_0V'(\rho_0)V''(\rho_0) + 6c_0^2f''(\rho_0)}\right],$$

for which Eq. (9) reads

$$\frac{\partial u}{\partial x_0}\frac{dx_0}{dt_1} + A\hat{\rho}_1 = -\left[\frac{2\tau\rho_0}{\mu}\alpha u_{xx} + \rho_0 u_{xxxx} + a(uu_x)_x\right].$$

Multiplying both sides by $\partial u/\partial x_0$ and integrating over x, we also get $dx_0/dt_1 = 0$, and obtain the equation of motion for $\hat{\rho}_1(x,t)$:

$$\frac{\partial}{\partial t}\hat{\rho}_1(x,t) = \frac{\partial^3}{\partial x^3}\hat{\rho}_1(x,t) + 6u\frac{\partial}{\partial x}\hat{\rho}_1(x,t) + 6u_x\hat{\rho}_1(x,t) - \epsilon\left[\frac{2\tau\rho_0\alpha}{\mu}u_{xx} + \rho_0u_{xxxx} + a(uu_x)_x\right], \quad (10)$$

which has the asymptotic form for $t \gg 1$:

$$\frac{\partial}{\partial t}\hat{\rho}_1(x,t) = \frac{\partial^3}{\partial x^3}\hat{\rho}_1(x,t). \quad (11)$$

It is thus obvious that the first-order correction $\hat{\rho}_1(x,t)$ does not lead to chaotic behavior.

We next consider the second-order corrections

$$\hat{\rho} = u + \epsilon\hat{\rho}_1 + \epsilon^2\hat{\rho}_2, \quad (12)$$

which, upon substituting in Eq. (6), yields the equation of motion for $\hat{\rho}_2$:

$$\left[\frac{\partial}{\partial t} - \frac{\partial^3}{\partial x^3} - 6\frac{\partial}{\partial x}u\right]\hat{\rho}_2(x,t) = 6\hat{\rho}_1\hat{\rho}_{1x} - \frac{3\mu}{2\tau V'(\rho_0)[2V'(\rho_0)+\rho_0V''(\rho_0)]}u_{xxx}u_x + \frac{9\mu V''(\rho_0)}{2\tau V'(\rho_0)[2V'(\rho_0)+\rho_0V''(\rho_0)]^2}u^2u_{xx} - \frac{2\tau\rho_0}{\mu}\alpha\hat{\rho}_{1xx} - \rho_0\hat{\rho}_{1xxxx} - a(\hat{\rho}_1\hat{\rho}_{1x})_x.$$

Thus the asymptotic behavior of $\hat{\rho}_2(x,t)$ is described by the equation

$$\frac{\partial}{\partial t}\hat{\rho}_2 - \frac{\partial^3}{\partial x^3}\hat{\rho}_2 = 6\hat{\rho}_1\hat{\rho}_{1x} - \frac{2\tau\rho_0}{\mu}\alpha\hat{\rho}_{1xx} - \rho_0\hat{\rho}_{1xxxx} - a(\hat{\rho}_1\hat{\rho}_{1x})_x \quad (13)$$

together with Eq. (11). From the time evolution of $\hat{\rho}_2$, which is obtained by numerical integration, we measure the asymptotic value of the Lyapunov exponent and obtain the value $\tilde{\lambda} = 1.25 \pm 0.27$ for $\rho_0 = c_0 = 0.35$. Thus the Lyapunov exponent associated with the second-order correction $\hat{\rho}_2$ is positive, and the corresponding instability induces chaotic behavior. In the original time scale, this corresponds to the Lyapunov exponent $\lambda = \mu\tilde{\lambda}/8\tau^2V'(\rho_0)^2 = 0.09 \pm 0.01$, which is in reasonable agreement with the value obtained from Fig. 1(a).

IV. CONCLUSION

We have studied the traffic problem in the hydrodynamic limit, which is described by the Navier-Stokes

equation together with the continuity equation. Particular emphasis has been paid to the cutoff in the traffic density, which is introduced to account for the granular nature of cars. We have computed the Lyapunov exponent associated with the time evolution of the system, which allows us to identify the chaotic phase and the density-wave phase. The phase diagram on the (ρ_0, c_0) plane exhibits the homogeneous phase with the laminar flow, the chaotic phase with the irregular flow, and the density-wave phase with traveling density waves, depending on the form of the average velocity relaxation profile $V(\rho)$. The power spectra of the current fluctuations are also computed, and found to display $1/f$ fluctuations in the density-wave phase; the latter appears when cars tend to persist their speed until they reach the cutoff. If the cars tend to slow down sufficiently before they reach the cutoff, the system does not display $1/f$ fluctuations. Instead the spectrum appears to be white, which is a characteristic of chaotic behavior. This suggests that the density-wave phase is not so robust against random fluctuations; the latter tends to produce chaotic evolution displaying the white spectrum. Still the chaotic behavior appears rather slowly, as implied by the small value of the Lyapunov exponent, and the density-wave behavior may seem to persist in the nonasymptotic regime. Such slow appearance of the chaotic behavior out of the density-wave behavior has been examined via the long-wave analysis, which shows that higher-order corrections to the soliton solution of the traffic equation give rise to the chaotic behavior.

ACKNOWLEDGMENTS

We thank S. Kim for useful discussions and help in obtaining figures. This work was supported in part by the SNU-Daewoo Research Fund, by the Basic Science Research Institute Program, Ministry of Education, and by the Korea Science and Engineering Foundation through the SRC Program.

[1] T. Musha and H. Higuchi, Jpn. J. Appl. Phys. **15**, 1271 (1976).

[2] P. Duta and P.M. Horn, Rev. Mod. Phys. **53**, 497 (1981); M.B. Weissman, *ibid.* **60**, 537 (1988).

[3] K. Nagel and M. Schreckenberg, J. Phys. (France) I **2**, 2221 (1992); O. Biham, A.A. Middleton, Phys. Rev. A **46**, R6124 (1992); A. Schadschneider and M. Schreckenberg, J. Phys. A **26**, L679 (1993); K. Nagel and H.J. Herrmann, Physica (Amsterdam) **199A**, 254 (1993).

[4] T. Nagatani, J. Phys. A **26**, L781; J. Phys. Soc. Jpn. **63**, 52 (1994); E. Ben-Naim, P.L. Krapivsky, and S. Render, Phys. Rev. E **50**, 822 (1994).

[5] G.B. Whitham, *Linear and Nonlinear Wave* (Wiley, New York, 1974); W. Leutzbach, *Introduction to the Theory of Traffic Flow* (Springer-Verlag, Berlin, 1988); *Highway Capacity and Level of Service*, edited by U. Brannolte (Balkema, Rotterdam, 1991).

[6] B.S. Kerner and P. Konhäuser, Phys. Rev. E **48**, R2335 (1993); **50**, 54 (1994).

[7] D.A. Kurze and D.C. Hong, Phys. Rev. E **52**, 218 (1995).

[8] D.C. Hong, S. Yu, J.K. Rudra, M.Y. Choi, and Y.W. Kim, Phys. Rev. E **50**, 4123 (1994).

[9] G. Peng and H.J. Herrmann, Phys. Rev. E **49**, R1796 (1994).

[10] W.H. Press, B.P. Flannery, S.A. Teukolsky, and W.T. Vetterling, *Numerical Recipes in C* (Cambridge University Press, Cambridge, 1988).

[11] C.G. Gardner, J.M. Green, M.D. Kruskal, and R.M. Miura, Phys. Rev. Lett. **19**, 1095 (1967).